analytical chemistry

Article

pubs.acs.org/ac

"Off-On" Electrochemiluminescence System for Sensitive Detection of ATP via Target-Induced Structure Switching

Yueting Liu, Jianping Lei, Yin Huang, and Huangxian Ju*

State Key Laboratory of Analytical Chemistry for Life Science, School of Chemistry and Chemical Engineering, Nanjing University, Nanjing 210093, P.R. China

ABSTRACT: An "off-on" electrochemiluminescence (ECL) strategy was constructed for highly sensitive and selective detection of adenosine 5′-triphosphate (ATP) with a quantum dots (QDs) modified electrode and a DNAzyme signal probe. The immobilized QDs were functionalized with a DNA sequence (DNA1) and then aptamer for recognition of target analyte. The signal probe was prepared by assembling another DNA sequence (DNA2) and G-quadruplex on gold nanoparticle via Au−S chemistry, which was used to bind the probe to electrode surface through a hybridization reaction with aptamer and hemin for forming G-quadruplex/hemin DNAzyme, respectively. Upon the sandwich hybridization of DNA1-aptamer-DNA2, the signal probe could be captured on the aptasensor to catalyze the reduction of dissolved oxygen, the coreactant for cathodic ECL emission of QDs, leading to a decrease of ECL intensity and thus the "off" state. In the presence of target, its recognition by aptamer led to the release of aptamer from electrode surface and decreased the amount of captured signal probe, thus the ECL emission was in its "on" state. The "off-on" strategy resulted from the target-induced structure switching could be used for specific detection of ATP with a linear range of 8−2000 nM and a detection limit of 7.6 nM. The proposed aptasensor could be successfully applied in the ECL detection of ATP in human serum. This method could resist environmental interfering agents and be extended for sensitive and reliable detection of a wide range of analytes in complex sample.

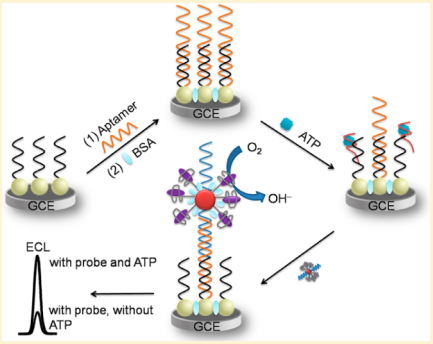

As the primary energy currency, adenosine 5′-triphosphate (ATP) plays an important role in many biological processes such as regulating cellular metabolism[1] and biochemical pathways.[2] The level of ATP can be an indicator for many diseases such as hypoxia, hypoglycemia, ischemia, Parkinson's disease, and some malignant tumors.[3] Therefore, exploring a reliable and sensitive method for specific detection of ATP is encouraging. Up until now, various methods have been designed for the detection of ATP including enzymatic cycling,[4−6] protein regulating,[7] and aptamer-based strategies.[8−13] In particular, the aptamer-based biosensing has become a hotspot due to the high binding affinity and specificity as well as structural switching property of aptamer and facile combination with amplification strategy. Herein, we designed an "off-on" electrochemiluminescence (ECL) aptasensing strategy by using aptamer to form a sandwich structure and target ATP to achieve the structure switching. The introduction of sandwich structure avoided the direct recognition of target to probe, thus decreased the effect of background noise.[14]

ECL has attracted increasing concern owing to its intrinsic advantages of high sensitivity, good stability, and low background.[15,16] Especially, the aptamer-based ECL methods have extensively been applied in the biosensing field.[17−21] For example, a "signal-off" aptasensor for the detection of ATP has been developed with the rule of Watson−Crick base pairing,[20] and a "signal-on" aptasensor has been proposed for the detection of Ramos cells.[21] Despite their advantages, these "signal-off" or "signal-on" ECL aptasensors may induce false positive signals due to the disassembly of the aptamer resulting from interfering agents, which limits their application in analysis of real samples. Thus, this work proposed an "off-on" ECL system by using G-quadruplex/hemin wrapped gold nanoparticles (AuNPs) as a signal probe to quench the ECL signal and aptamer-involved sandwich structure as the signal switch to produce an "on" state of ECL emission. The efficient quenching led to a very low-level "off" state, thus greatly improved the sensitivity.

G-quadruplex/hemin, as enzyme mimics, has attracted immense research attention in biosensing due to its high chemical stability, low cost, and simple synthesis.[22−24] On the basis of the catalytic activity toward the reduction of H_2O_2 or dissolved oxygen, it has been widely used as a signal amplifier to construct biosensors for metal ions,[23−27] small biomolecules,[28,29] DNA,[30,31] and protein.[32,33] This work utilized its strong catalytic ability toward the reduction of dissolved oxygen to achieve the quenching of ECL emission of quantum dots (QDs). Although the quenching mechanism and similar signal probe have been proposed for ECL "signal off" immunoassay in our previous work,[32] this work used an aptamer-specific target to decrease the amount of captured signal probe and thus produced an "on" state of the ECL emission. Furthermore, by

Received: May 21, 2014
Accepted: August 13, 2014
Published: August 13, 2014

   dx.doi.org/10.1021/ac501913c | *Anal. Chem.* 2014, 86, 8735−8741

introducing a sandwich structure to separate the assembly of the aptamer, the recognition of aptamer to target and the capture of signal probe, the false positive signals resulting from interfering agents could be excluded.

As shown in Scheme 1, the sandwich structure was formed by two hybridization reactions between a DNA sequence

Scheme 1. Schematic Illustration of "Off-On" Electrochemiluminesce Biosensing System via Target-Induced Structure Switching

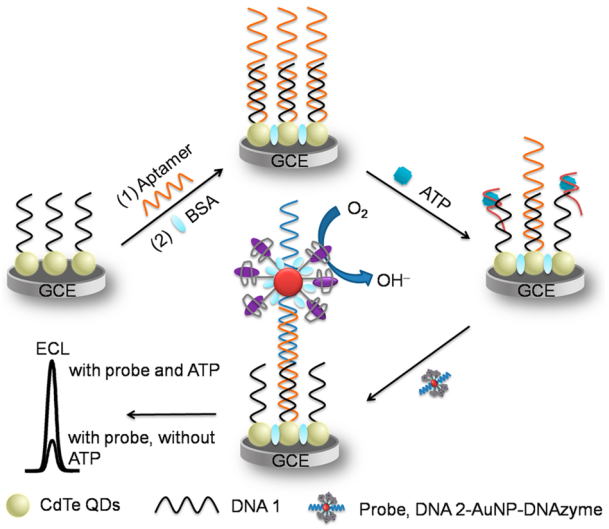

(DNA1) immobilized on QDs modified electrode and aptamer, and then the aptamer and signal probe modified with another DNA sequence (DNA2) that was complementary to another end of the aptamer. In the presence of target ATP, the binding of ATP with aptamer led to the disassembly of the aptamer, and thus the low loading of signal probe at the electrode surface, which achieved the target-induced structure switching and thus increased the ECL signal. The increase of ECL signal depended on the concentration of target ATP. The proposed method could detect ATP down to the nanomolar level. This "off-on" strategy has been successfully applied in the direct detection of ATP in human serum and possessed its potential application in bioanalysis and clinical diagnosis.

EXPERIMENTAL SECTION

Reagents and Materials. Bovine serum albumin (BSA), hemin, tri(2-carboxyethyl) phosphine hydrochloride (TCEP), *N*-hydroxysulfosuccinimide (NHS), and 1-ethyl-3-(3-(dimethylamino)propyl) carbodiimide (EDC) were purchased from Sigma-Aldrich Chemical Co. (St. Louis, MO). Cadmium chloride ($CdCl_2 \cdot H_2O$) and meso-2,3-dimercaptosuccinic acid (DMSA) were purchased from Alfa Aesar China Ltd. (China). Trisodium citrate, chloroauric acid ($HAuCl_4 \cdot 3H_2O$), and sodium hydroxide were purchased from Sinopharm Co. Ltd. (Shanghai, China). Tellurium rod was purchased from Leshan Kayada Photoelectricity Co. (China). ATP, guanosine triphosphate (GTP), cytidine triphosphate (CTP), and uridine triphosphate (UTP) were obtained from Sangon Biological Engineering Technology & Services Co. Ltd. (Shanghai, China). Human serum samples were obtained from Jiangsu Institute of Cancer Prevention and Cure. All other reagents were of analytical grade and used as received. Ultrapure water obtained from a Millipore water purification system (≥18 MΩ, Milli-Q, Millipore) was used in all assays. Phosphate buffer saline (PBS, 0.1 M pH 9.0) was used as the detection solution and was prepared by mixing the stock solutions of NaH_2PO_4 and Na_2HPO_4 containing 0.1 M KNO_3. PBS (10 mM pH 7.4) containing 0.1 M NaCl was used as the coupling buffer and washing buffer.

The synthetic single-stranded oligonucleotides were purchased from Sangon Biological Engineering Technology & Services Co., Ltd. (Shanghai, China) and purified using high-performance liquid chromatography. Their sequences were given below:

DNA1: 5′-**CCCAGGTAACAAGA**TTTTT-$(CH_2)_7$-NH_2-3′

Aptamer: 5′-**TCTTGTTACCTGGG***GGAGTATTGCGGAGGAAGGT*-3′

DNA2: 5′-SH-$(CH_2)_6$-TTTTT*ACCTTCCTCCGCAATACTCC*-3′

G-quadruplex: 5′-TGGGTAGGGCGGGTTGGGTTTTTT-$(CH_2)_6$-SH-3′

1-mismatched DNA: 5′-TCTTGTTACCTGG**C**GGAGTATTGCGGAGGAAGG-3′

2-mismatched DNA: 5′-TCTTGTTACCTGG**C**GG**T**GTATTGCGGAGGAAGG-3′

Apparatus. The electrochemical experiments were performed on a CHI 812B electrochemical workstation (CH Instruments Inc.). ECL measurements were carried out on a MPI-E multifunctional electrochemical and chemiluminescent analytical system (Xi'an Remex Analytical Instrument Ltd. Co., China). All experiments were carried out with a conventional three-electrode system. The working electrode was a modified glassy carbon electrode (GCE, 5 mm in diameter), Pt wire, and an Ag/AgCl (saturated KCl) electrode served as the counter and reference electrodes, respectively. The ECL emission window was placed in front of the photomultipier tube (PMT, detection range from 300 to 650 nm) biased at 1000 V.

The ultraviolet−visible (UV−vis) absorption spectra were recorded with a Nanodrop-2000C UV−vis spectrophotometer (Nanodrop). The photoluminescent (PL) experiment was performed on a RF-5301 PC fluorometer (Shimadzu Co., Japan). The transmission electron micrographs (TEM) were obtained using a JEM-2100 TEM instrument (JEOL, Japan). The circular dichroism (CD) spectra were conducted on JASCO J-810-150S circular spectropolarimeter (Tokyo, Japan), of which the lamp was always kept under a stable stream of dry purified nitrogen (99.99%) during experiments. Electrochemical impedance spectroscopic (EIS) measurements were carried out on a PGSTAT30/FRA2 system (Autolab, The Netherlands) in 0.1 M KNO_3 containing 5 mM $K_3[Fe(CN)_6]$/$K_4[Fe(CN)_6]$.

Preparation of Signal Probe. AuNPs with 13 nm diameter and the signal probe were prepared according to the previous report[32] with minor modification. Briefly, the mixture of DNA2 (1.5 μL, 100 μM) and G-quadruplex (7.5 μL, 100 μM) was activated with 0.5 μL of 100 mM TCEP to reduce disulfide bonds and then mixed with 500 μL of 10 nM AuNPs solution containing 0.01% tween-20 to incubate for 16 h with stirring at room temperature, which produced G-quadruplex and DNA2 modified AuNPs (DNA2-AuNP-G-quadruplex). Followed by a salt-stabilization in 0.1 M NaCl, 1% BSA was added to the resulting solution to block the active surface of AuNPs. The excess DNA and BSA were removed by centrifugation (12 000 rcf, 30 min, 4 °C). The obtained precipitate was redispersed in 500 μL of 0.01 M PBS containing 0.1 M KCl. Finally, 10.0 μL of 100 μM hemin was added to the

dx.doi.org/10.1021/ac501913c | *Anal. Chem.* 2014, 86, 8735−8741

suspension and incubated for 2 h in the dark to form a DNA2-AuNP-DNAzyme probe, and the redundant hemin was removed by centrifugation (12 000 rcf, 20 min, 4 °C). The signal probe was kept in 0.01 M PBS containing 0.1 M KCl at 4 °C prior to use.

Fabrication of ECL Aptasensor. Prior to sensor fabrication, the GCE was polished to a mirror using 1.0 and 0.05 μm alumina slurry (Beuhler) followed by sonication in water, ethanol, and water, respectively. The electrode was rinsed with water and allowed to dry at room temperature. The water-soluble CdTe QDs were prepared using DMSA as a stabilizing agent according to the electrolysis method.[34] A volume of 200 μL of as-prepared QDs solution was mixed with 200 μL of isopropyl alcohol and centrifuged at 8000 rcf for 5 min. Decanting the supernatant, the precipitation was dissolved in 20 μL of water and dropped onto the GCE. After dried in air at room temperature, the carboxylic group on the surface was activated using 10 mM EDC and 20 mM NHS solutions in PBS (pH 5.5) for 50 min. Afterward, the electrode was washed, and 10.0 μL of DNA1 (0.1 μM) was dropped onto its surface to incubate at 4 °C overnight. After the electrode was washed thoroughly to remove the unlinked DNA1, 10.0 μL of aptamer (40 nM) was dropped on the surface to incubate at 37 °C for 50 min. The resulting electrode was washed with PBS and blocked with 10.0 μL of 1% BSA for 50 min at room temperature. The prepared ECL aptasensor was kept at 4 °C.

Analytical Procedure. In a typical test, the prepared aptasensor was incubated with target ATP of different concentrations for 2 h at 37 °C, followed by thoroughly washing with PBS to remove unbound ATP and the disassembled aptamer-ATP conjugate. Then, 10.0 μL of the signal probe was dropped to the surface to react for 40 min at 37 °C. Subsequently, the electrode was washed thoroughly with PBS to remove unhybridized signal probe. Finally, the ECL signal was detected in air-saturated 0.1 M pH 9.0 PBS containing 0.1 M KNO_3.

Human serum samples were diluted 5-fold with PBS. The practical samples were spiked with various concentrations of ATP and analyzed in a manner similar to that described above.

RESULTS AND DISCUSSION

Viability of Strategy. The target-induced structure switching could be achieved by the competition between DNA1 and target to bind the aptamer. The latter resulted in the disassembly of aptamer on QDs modified electrode and thus decreased the amount of captured signal probe. The competitive binding could be observed with the CD spectra (Figure 1). Different from DNA1 (curve a) and aptamer (curve b), their mixture showed a positive band near 267 nm and a negative band at 241 nm (curve c), which were at shorter wavelengths than both DNA1and aptamer, confirming the formation of a B-form DNA duplex.[35] After ATP was added to the mixture, a significant change in the ellipticity was observed (curve d). The typical band of a B-form DNA duplex disappeared and a positive band near 285 nm and a negative band at 250 nm appeared, which were the typical characteristics of the ATP-aptamer structure,[36] indicating the configuration change upon the introduction of ATP. Therefore, the introduction of ATP led to the dehybridization of DNA1-aptamer duplex and thus induced the structure switching from B-form DNA duplex to aptamer-ATP complex, which provided a possibility for design of the proposed strategy.

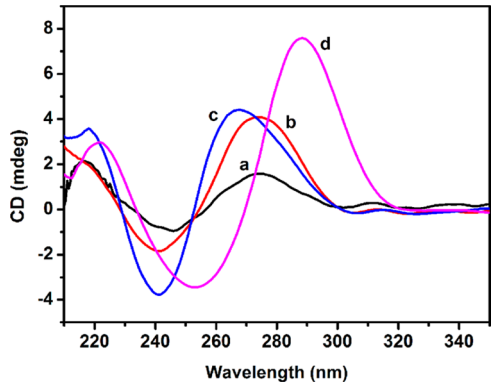

Figure 1. CD spectra of DNA1 (a), aptamer (b), the mixture of DNA1 and aptamer (c), and ATP added in part c (d). The concentration of DNA1, aptamer, and ATP were 5.0, 5.0, and 50 μM, respectively.

Characterization of QDs and Signal Probe. The CdTe QDs showed a broad excitation profile centered at 464 nm (Figure 2A, curve a) and narrow PL emission spectrum centered at 610 nm (λ_{ex} = 417 nm) (Figure 2A, curve b), which were similar to those reported previously.[34] The TEM image of QDs exhibited a homogeneously dispersion with an average size of 6 nm (Figure 2C). According to Peng's empirical equation,[37] the concentration of the QDs was estimated to be 0.25 μM.

The UV−vis absorption spectra were performed to characterize the signal probe (Figure 2B). The size of AuNPs could be estimated to be 13 nm from the absorption peak at 519 nm (curve a), which was further confirmed by TEM (Figure 2D). After assembling G-quadruplex and DNA2 on the surface, the obtained AuNPs exhibited a new characteristic absorbance of DNA at 260 nm and a red shift of the AuNP absorption peak (curve b), indicating their successful loading on AuNPs. After the G-quadruplex assembled on AuNPs bound hemin and then the AuNPs were blocked with BSA to form the signal probe, an absorption peak occurred at 276 nm (curve c), which was corresponding to the typical protein absorption. The concentration of signal probe was detected to be about 9.6 nM according to the absorbance of signal probe at 534 nm and molar absorptivity,[38] and the average surface coverage of the oligonucleotides on one probe was calculated to be 120, according to the absorbance of nontagged oligonucleotide in the supernate after centrifugation. The high loading of DNAzyme on AuNPs was beneficial to the high detection sensitivity.

Characterization of ATP Aptasensor. The stepwise fabrication of the ATP aptasensor was confirmed with ECL and EIS measurements. The QDs modified GCE showed an intensive ECL emission at −1.3 V in air-saturated pH 9.0 PBS (Figure 3A, curve a). After bound by DNA1, the ECL intensity slightly decreased (Figure 3A, curve b) due to the increased electron transfer resistance and repellence of negatively charged DNA 1 to $[Fe(CN)_6]^{3-/4-}$ (Figure 3B, curve b). Accompanied by the increase of electron transfer resistance, the ECL intensity gradually decreased with the further binding of DNA1 with aptamer (curve c) and blocking with BSA (curve d). After the aptasenor was incubated with the signal probe, an outstanding decline in ECL intensity was observed (curve f), which was much lower than that incubated with DNA2-AuNP-G-quadruplex (curve g), though they showed similar electron transfer resistance. This could be attributed to the efficient

dx.doi.org/10.1021/ac501913c | Anal. Chem. 2014, 86, 8735−8741

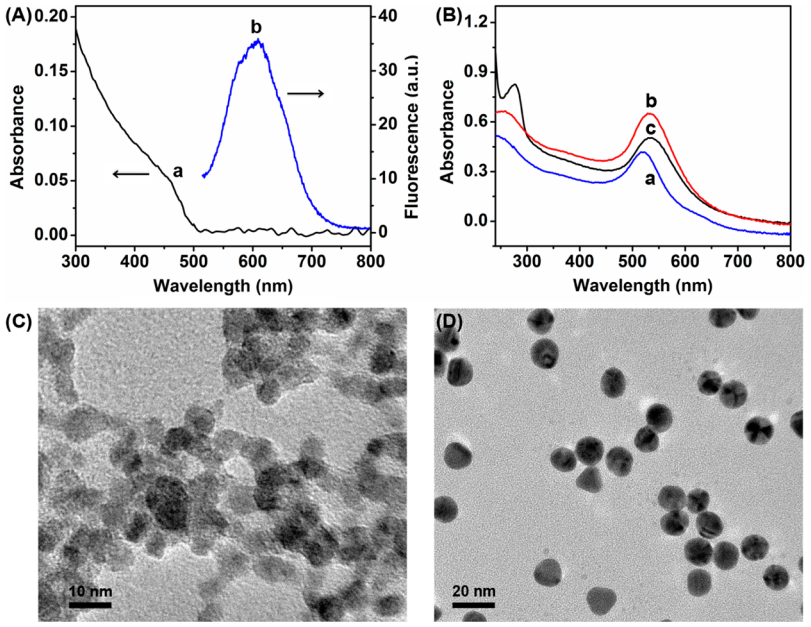

Figure 2. (A) UV−vis (a) and PL (b) spectra of CdTe QDs, (B) UV−vis spectra of AuNPs (a), DNA2-AuNP-G-quadruplex (b), and signal probe (c) in pH 7.4 PBS. TEM images of (C) CdTe QDs and (D) AuNPs.

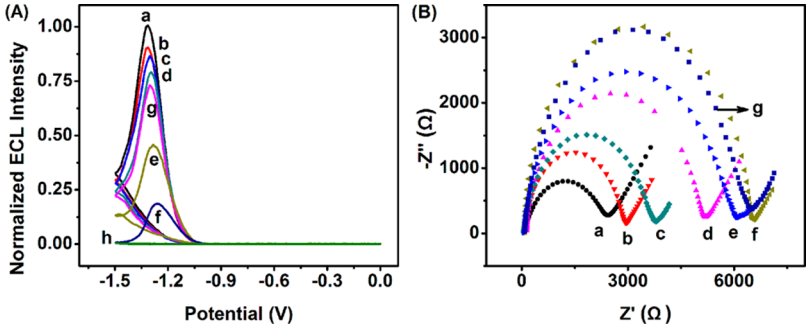

Figure 3. (A) ECL potential curves and (B) corresponding EIS of QDs (a), DNA1/QDs (b), aptamer/DNA1/QDs (c), aptasensor (d), signal probe/aptasensor in presence (e) and absence of 1.0 μM ATP (f), and DNA2-AuNP-G-quadruplex/aptasensor (g) in air-saturated 0.1 M pH 9.0 PBS, and (h) aptasensor in N_2-saturated 0.1 M pH 9.0 PBS.

catalytic reduction of dissolved oxygen by G-quadruplex/hemin DNAzyme on the probe.[34] After the aptasenor was incubated with 1.0 μM ATP and then the signal probe, the ECL emission showed significantly greater intensity than that in the absence of ATP (curves e and f). The difference resulted from the disassembly of aptamer due to the binding of ATP with aptamer, which decreased the loading of signal probe and the electron transfer resistance (Figure 3B, curve e), thus realized the "off-on" strategy.

"Off-On" Mechanism of ECL Emission. As described above, both the QDs modified electrode and the aptasenor showed strong ECL emission (Figure 3A, curves a and d). The dissolved oxygen could be considered as the coreactant of ECL emission as reported previously,[30] which was also confirmed by comparing the ECL responses of aptasensor in air- and N_2-saturated 0.1 M pH 9.0 PBS (Figure 3A, curves d and h). After DNA2-AuNP-G-quadruplex was captured by the aptasenor, the ECL intensity slightly decreased due to the increase of electron transfer resistance (Figure 3, from curve d to curve g). The much greater change of ECL intensity upon the capture of signal probe by the aptasenor (Figure 3, from curve d to curve f) was due to the reduction of coreactant dissolved oxygen, which could be observed from the cyclic voltammograms at around −0.56 V (Figure 4, curves a and c). Although the DNA2-AuNP-G-quadruplex captured aptasenor also showed a reduction peak of dissolved oxygen at −0.98 V (Figure 4, curves b and c), the electrochemical reduction product H_2O_2 could be used as the coreactant of ECL emission.[35] The reduction peak at −0.56 V could be ascribed to the catalytic reduction of O_2 by DNAzyme toward described as follows:[39]

$$\text{Fe(III)DNAzyme} + e^- \rightarrow \text{Fe(II)DNAzyme} \quad (1)$$

$$4\text{Fe(II)DNAzyme} + O_2 + 2H_2O \rightarrow 4\text{Fe(III)DNAzyme} + 4OH^- \quad (2)$$

The consumption of coreactant greatly prohibited the formation of the excited state CdTe* for ECL emission of QDs, leading to the "off" state. The "off" state could be avoided by the disassembly of aptamer from the aptasensor surface in the presence of target ATP, which achieved target-induced structure switching to produce the "on" state for detection of ATP.

Optimization of Detection Conditions. In coreactant-based ECL emission of QDs, the ECL intensity depends on the

dx.doi.org/10.1021/ac501913c | Anal. Chem. 2014, 86, 8735−8741

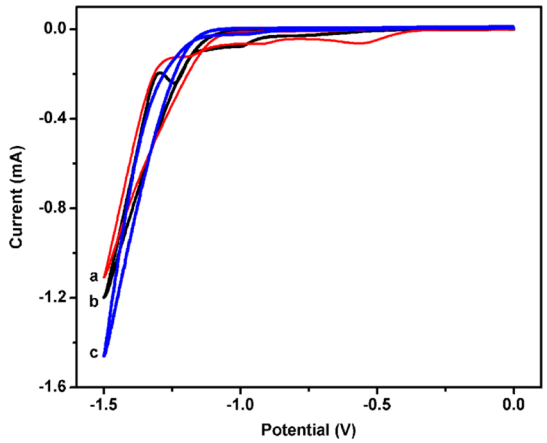

Figure 4. Cyclic voltammograms of DNA2-AuNP-G-quadruplex/aptasensor in the presence (a, c) and absence of hemin (b) in air-saturated (a, b) and N_2-saturated (c) 0.1 M pH 9.0 PBS containing 0.1 M KNO_3.

pH of the detection solution. As shown in Figure 5A, the ECL intensity of the aptasensor increased with the increasing pH value due to the better stability of the electrogenerated intermediates of dissolved O_2 at high pH. The quenching efficiency of signal probe reached the maximum at pH 9.0. Therefore, pH 9.0 was selected for following ECL measurements.

The concentration of aptamer for preparation of aptasensor affected greatly its sensitivity (Figure 5B). When the concentration of aptamer increased, the quenching efficiency increased drastically and reached a plateau at 40 nM, indicating a saturated capture of aptamer and thus the signal probe. Thus, 10.0 μL of 40 nM aptamer was chosen for the preparation of aptasensor.

The incubation times of the aptasensor with both signal probe and target ATP were further optimized. When the incubation time with signal probe increased, more signal probe was captured by the aptasensor, thus the quenching efficiency increased (Figure 5C). The quenching efficiency trended to the maximum value at 40 min, indicating the saturated capture of signal probe, so 40 min was used for incubation of signal probe. Similarly, with the increasing incubation time of the aptasensor with 200 nM ATP, the ECL intensity increased due to the less loading of signal probe during the followed 40 min incubation process (Figure 5D). A stable ECL intensity could be achieved at 2 h, which was chosen as the optimal condition.

When the ratio of G-quadruplex to DNA2 on one AuNP was 5:1, the ratio of signal-to-noise for 100 nM ATP reached the maximum value of 1.71, which was 1.7 and 1.3 times higher than those at the G-quadruplex-to-DNA2 ratios of 1:1 and 10:1 on one AuNP, respectively. Thus, the optimal ratio of G-quadruplex to DNA2 was 5:1.

Analytical Performance of ATP Aptasensor. Under the optimal conditions, the ECL intensity became larger with the increasing ATP concentration because more aptamer released from the sensor surface (Figure 6A). The calibration plot showed a good linear relationship between ECL intensity and the logarithmic value of ATP concentration ranging from 8 to 2000 nM, with a correlation coefficient of 0.996 (inset in Figure 6B). The detection limit was estimated to be 7.6 nM at 3σ, which was much lower than those previously reported detection of ATP without amplification.[11,12]

Nine measurements of ECL emission upon cyclic scans of the ATP aptasensor in the presence and absence of 1 μM ATP is shown in Figure 6C, which showed the relative standard deviations (RSD) of 2.0% and 2.1% for ECL measurements, respectively, indicating quite satisfying stability. The interassay precision of the ATP aptasensor was examined at 1.0 μM target for five times, which showed a RSD of 2.6%. Thus, the precision and fabrication reproducibility were acceptable. The long-time stability of the constructed aptasensor was examined with 100 nM ATP as the detection sample, and the aptasensor was kept at 4 °C when it was not in use. The ECL intensity did

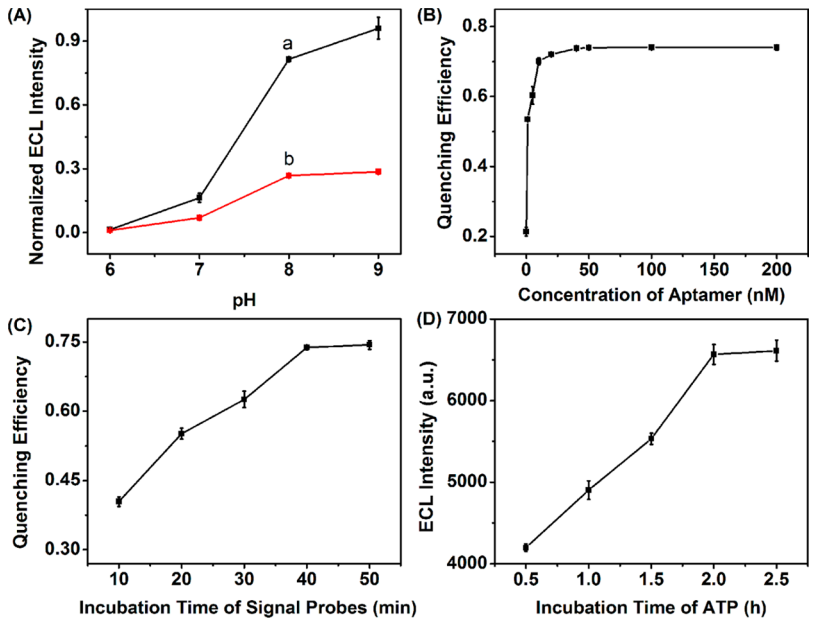

Figure 5. Effects of (A) pH of detection solution before (a) and after (b) incubation with signal probe, (B) concentration of aptamer, (C) incubation time for signal probe, and (D) incubation time for ATP on ECL response of aptasensor in air-saturated PBS in absence (A, B, C) and presence (D) of 200 nM ATP.

dx.doi.org/10.1021/ac501913c | *Anal. Chem.* 2014, 86, 8735−8741

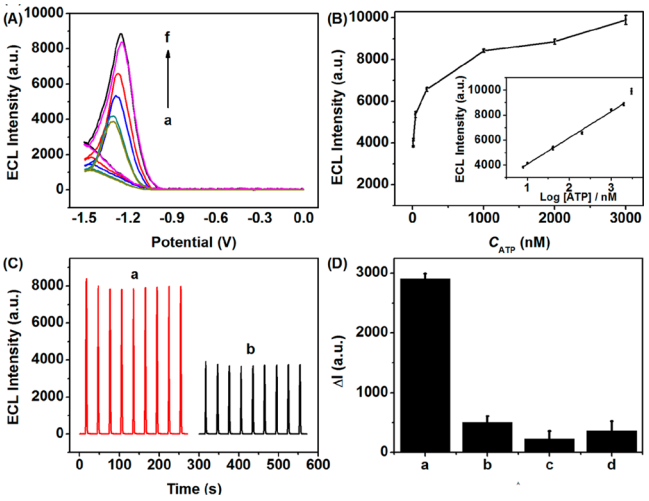

Figure 6. (A) ECL-potential curves of aptasensor at 8, 10, 40, 200, 1000, and 2000 nM ATP (from a to f). (B) Plot of ECL intensity vs ATP concentration. Inset: calibration curve. (C) Continuous cyclic ECL scans of the aptasensor in the presence (a) and absence (b) of 1000 nM ATP. (D) ECL responses of the aptasensor to 200 nM ATP (a), 2000 nM GTP (b), CTP (c), and UTP (d).

not show an obvious change after the aptasensor was stored for 1 week and decreased only 5% after 2 weeks. Thus, the long-time stability of the constructed aptasensor was acceptable.

Selectivity of ATP Aptasensor. To investigate the binding specificity of the ECL aptasensor, the ECL intensity changes upon incubation with ATP and other compounds such as CTP, GTP, and UTP were measured. The changes resulted from three analogues were one-fifth less than that with ATP, even if their concentrations were 10-fold higher than ATP (Figure 6D, columns a–d). It suggested that the proposed method was of excellent specificity.

Detection of ATP in Complex Samples. The proposed aptasensor was used for the detection of ATP in human serum samples. With a standard addition method, the ATP levels in two human serum samples were detected to be 0.91 μM and 0.93 μM, respectively, which was similar to the result obtained with the reported method.[40] After these serum samples were spiked with 200 nM and 400 nM ATP, the recoveries for three detections were 92.8% ± 7.3% and 98.4% ± 6.4% for 200 nM ATP and 97.4% ± 6.8% and 96.5% ± 7.9% for 400 nM ATP, respectively, indicating acceptable accuracy. It demonstrated that this method could be used for quantification of ATP in complex biological fluids.

CONCLUSION

An "off-on" ECL strategy has been designed for highly sensitive and selective detection of ATP by using G-quadruplex/hemin wrapped AuNPs as a signal probe and aptamer-involved sandwich structure as the signal switch on QDs modified electrode. The signal probe is an efficient quenching probe to the ECL emission due to the high loading of DNAzyme for catalytic reduction of coreactant dissolved oxygen. The target-induced structure switching leads to the disassembly of aptamer, which decreases the loading of signal probe and forms the "on" state for detection of target ATP. The ATP aptasensor shows high sensitivity, excellent specificity and acceptable precision, and fabrication reproducibility and has been applied in analysis of ATP in real samples. The proposed method provides a proof-of-concept of "off-on" ECL strategy for reliable detection of a wide range of analytes in practice.

AUTHOR INFORMATION

Corresponding Author

*Phone/fax: +86-25-83593593. E-mail: hxju@nju.edu.cn.

Notes

The authors declare no competing financial interest.

ACKNOWLEDGMENTS

We gratefully acknowledge the National Basic Research Program (Grant 2010CB732400) and National Natural Science Foundation of China (Grants 21135002 and 21121091).

REFERENCES

(1) Llaudet, E.; Hatz, S.; Droniou, M.; Dale, N. *Anal. Chem.* **2005**, *77*, 3267–3273.
(2) Wang, J.; Jiang, Y. X.; Zhou, C. S.; Fang, X. H. *Anal. Chem.* **2005**, *77*, 3542–3546.
(3) Gourine, A. V.; Llaudet, E.; Dale, N.; Spyer, K. M. *Nature* **2005**, *436*, 108–111.
(4) Lu, L. M.; Zhang, X. B.; Kong, R. M.; Yang, B.; Tan, W. H. *J. Am. Chem. Soc.* **2011**, *133*, 11686–11691.
(5) Xue, Q. W.; Wang, L.; Jiang, W. *Chem. Commun.* **2013**, *49*, 2640–2642.
(6) Zhang, Z. X.; Balogh, D.; Wang, F.; Willner, I. *J. Am. Chem. Soc.* **2013**, *135*, 1934–1940.
(7) Berg, J.; Hung, Y. P.; Yellen, G. *Nat. Methods* **2009**, *6*, 161–166.
(8) He, X. X.; Zhao, Y. X.; He, D. G.; Wang, K.; Xu, F. Z.; Tang, J. L. *Langmuir* **2012**, *28*, 12909–12915.
(9) Wang, L.; Xu, M.; Han, L.; Zhou, M.; Zhu, C. Z.; Dong, S. J. *Anal. Chem.* **2012**, *84*, 7301–7307.
(10) Zhao, W. A.; Chiuman, W.; Lam, J. C. F.; McManus, S. A.; Chen, W.; Cui, Y. G.; Pelton, R.; Brook, M. A.; Li, Y. F. *J. Am. Chem. Soc.* **2008**, *130*, 3610–3618.
(11) Li, F.; Du, Z. F.; Yang, L. M.; Tang, B. *Biosens. Bioelectron.* **2013**, *41*, 907–910.
(12) Li, J.; Fu, H. E.; Wu, L. J.; Zheng, A. X.; Chen, G. N.; Yang, H. H. *Anal. Chem.* **2012**, *84*, 5309–5315.
(13) Tan, X. H.; Chen, T.; Xiong, X. L.; Mao, Y.; Zhu, G. Z.; Yasum, E.; Li, C. M.; Zhu, Z.; Tan, W. H. *Anal. Chem.* **2012**, *84*, 8622–8627.
(14) Goldman, J. M.; Zhang, L. A.; Manna, A.; Armitage, B. A.; Ly, D. H.; Schneider, J. W. *Biomacromolecules* **2013**, *14*, 2253–2261.
(15) Richter, M. M. *Chem. Rev.* **2004**, *104*, 3003–3036.
(16) Dini, D. *Chem. Mater.* **2005**, *17*, 1933–1945.
(17) Yin, X. B.; Xin, Y. Y.; Zhao, Y. *Anal. Chem.* **2009**, *81*, 9299–9305.
(18) Wang, J.; Shan, Y.; Zhao, W. W.; Xu, J. J.; Chen, H. Y. *Anal. Chem.* **2011**, *83*, 4004–4011.
(19) Zhang, J.; Chen, P. P.; Wu, X. Y.; Chen, J. H.; Xu, L. J.; Chen, G. N.; Fu, F. F. *Biosens. Bioelectron.* **2011**, *26*, 2645–2650.
(20) Huang, H. P.; Tan, Y. L.; Shi, J. J.; Liang, G. X.; Zhu, J. J. *Nanoscale* **2010**, *2*, 606–612.
(21) Nie, G. M.; Bai, Z. M.; Yu, W. Y.; Chen, J. *Biomacromolecules.* **2013**, *14*, 834–840.
(22) Pelossof, G.; Tel-Vered, R.; Elbaz, J.; Willner, I. *Anal. Chem.* **2010**, *82*, 4396–4402.
(23) Pelossof, G.; Tel-Vered, R.; Willner, I. *Anal. Chem.* **2012**, *84*, 3703–3709.
(24) Yin, B. C.; Ye, B. C.; Tan, W. H.; Wang, H.; Xie, C. C. *J. Am. Chem. Soc.* **2009**, *131*, 14624–14625.
(25) Zhou, X. H.; Kong, D. M.; Shen, H. X. *Am. Chem.* **2010**, *82*, 789–793.
(26) Lin, J.; Yan, Y. Y.; Ou, T. M.; Tan, J. H.; Huang, S. L.; Li, D.; Huang, Z. S.; Gu, L. Q. *Biomacromolecules* **2010**, *11*, 3384–3389.
(27) Qin, H. X.; Ren, J. T.; Wang, J. H.; Luedtke, N. W.; Wang, E. K. *Anal. Chem.* **2010**, *82*, 8356–8360.

(28) Zhu, J. B.; Zhang, L. B.; Zhou, Z. X.; Dong, S. J.; Wang, E. K. *Anal. Chem.* **2014**, *86*, 312−316.
(29) Li, D.; Shlyahovsky, B.; Elbaz, J.; Willner, I. *J. Am. Chem. Soc.* **2007**, *129*, 5804−5805.
(30) Deng, S. Y.; Cheng, L. X.; Lei, J. P.; Cheng, Y.; Huang, Y.; Ju, H. X. *Nanoscale* **2013**, *5*, 5435−5441.
(31) Gao, Y.; Li, B. X. *Anal. Chem.* **2013**, *85*, 11494−11500.
(32) Lin, D. J.; Wu, J.; Yan, F.; Deng, S. Y.; Ju, H. X. *Anal. Chem.* **2011**, *83*, 5214−5221.
(33) Zhao, X. Q.; Wu, J.; Liang, J. H.; Yan, J. W.; Zhu, Z.; Yang, C. J.; Mao, B. W. *J. Phys. Chem. B* **2012**, *116*, 11397−11404.
(34) Cheng, L. X.; Liu, X.; Lei, J. P.; Ju, H. X. *Anal. Chem.* **2010**, *82*, 3359−3364.
(35) VorlíčKová, M.; Kejnovská, I.; Bednářová, K.; Renčiuk, D.; Kypr, J. *Chirality* **2012**, *24*, 691−698.
(36) Tang, W.; Wang, H. M.; Wang, D. Z.; Zhao, Y.; Li, N.; Liu, F. *J. Am. Chem. Soc.* **2013**, *135*, 13628−13631.
(37) Yu, W. W.; Qu, L. H.; Guo, W. Z.; Peng, X. G. *Chem. Mater.* **2003**, *15*, 2854−2860.
(38) Hasis, W.; Thanh, N. T. K.; Aveyard, J.; Fernig, D. G. *Anal. Chem.* **2007**, *79*, 4215−4221.
(39) Zheng, N.; Zeng, Y.; Osborne, P. G.; Li, Y.; Chang, W.; Wang, Z. *J. Appl. Electrochem.* **2002**, *32*, 129−133.
(40) Liu, J. H.; Wang, C. Y.; Jiang, Y.; Hu, Y. P.; Li, J. S.; Yang, S.; Li, Y. H.; Yang, R. H.; Tan, W. H.; Huang, C. Z. *Anal. Chem.* **2013**, *85*, 1424−1430.